Nuclear Magnetic Resonance Studies of Blends Containing Poly(ethylene terephthalate) (PET) and Poly(*p*-hydroxybenzoic acid-*co*-*p*-hydroxynaphthoic acid) (Vectra-A)

Pei Tang, Jeffrey A. Reimer,* and Morton M. Denn

Center for Advanced Materials, Lawrence Berkeley Laboratory, and Department of Chemical Engineering, University of California, Berkeley, California 94720-9989

Received March 8, 1993; Revised Manuscript Received April 20, 1993

ABSTRACT: Solid-state NMR techniques are used to characterize the interfacial interactions and morphology in Vectra-A/PET blends. Two-dimensional rotor-driven ^{13}C spin diffusion NMR and indirect detection of ^{1}H spin–lattice relaxation (T_1) are used to determine the extent of intimate molecular mixing, carbon-13 magic angle spinning line shapes emanating from methylene carbons in PET are used to monitor the conformation of PET in the blends, and indirect detection of ^{1}H spin–lattice relaxation in the rotational frame ($T_{1\rho}$) is used to estimate the polymer crystallinity. The results are presented in terms of a scenario in which Vectra can penetrate PET regions in blends upon annealing in the melt. This scenario accounts well for previously published thermal data.

Introduction

Blends of thermotropic liquid crystalline polymers (LCPs) with flexible engineering polymers are of interest for several reasons. Small amounts of LCP dispersed in a flexible polymer matrix can improve "processibility", and elongated inclusions of LCP in a conventional engineering plastic can lead to improved overall mechanical properties. The possible advantages of using LCPs in blends have been discussed in a recent National Research Council report.[1] Literature results detailing the effects of temperature, composition, and shear on the morphology and properties of blends of LCPs with flexible polymers are reviewed in ref 2, with more recent references in refs 3 and 4.

Blends of perfectly rigid and flexible polymers are thermodynamically incompatible. The conformation of melt-processible LCPs, however, is not rigid, even though long persistence lengths are expected because of the molecular architecture. Thus one might expect interactions between separated phases in LCP/flexible polymer blends. Indeed, previous studies[5] have shown that the presence of a liquid crystalline polyester can accelerate the rate of crystallization of poly(ethylene terephthalate) (PET), a thermoplastic polymer, in a manner similar to that of nucleating agents and can also affect the crystal structure of PET in the blends. It was also found under some blending conditions that the LCP penetrated into the thermoplastic polymer phase to enhance the interactions between the two blended polymers. Previous workers[6] have also shown that when blending polycarbonate with certain liquid crystalline polymers, the LCP can exist in the polycarbonate–rich phase, while polycarbonate is excluded from the LCP-rich phase. Annealing in the melt apparently caused transesterification between the chains and thus improved miscibility.

A previous study[3] on annealed blends of PET with Vectra-A, a random copolyester containing 73% *p*-hydroxybenzoic acid (HBA) and 27% hydroxynaphthoic acid (HNA) manufactured by Hoechst Celanese, showed depression of both the PET melting temperature, T_m, and crystallization temperature, T_c, with increasing Vectra content. The extent of this depression increases with annealing time. Similar phenomena were also reported[7] in a Vectra/PET blend containing 75% Vectra. Furthermore, the addition of small amounts of Vectra to the PET caused a decrease in viscosity below that of either pure component. It is these studies of Vectra/PET blends which motivate the present work.

Solid-state NMR has proven to be a powerful tool for the characterization of polymer blend morphology and miscibility. It is complementary to other techniques in providing detailed information about interactions at the molecular level. Cross polarization between deuterated and protonated polymers in blends has been used successfully to determine miscibility at length scales on the order of 1 nm or less.[8] One- and two-dimensional proton spin diffusion NMR spectroscopy has been used to estimate the domain sizes in semicrystalline and crystalline polymers.[9] The crystallinity of the blended polymers can be determined based on changes in the spin relaxation behaviors, because alterations in morphology are normally associated with changes in molecular dynamics and thus reflected as changes in spin relaxation rates.

In the present study, solid-state NMR is applied to characterize the interfacial interactions and morphology in Vectra-A/PET blends. Two-dimensional rotor-driven ^{13}C spin diffusion NMR and indirect detection of ^{1}H spin–lattice relaxation (T_1) are used to determine the mixing of Vectra and PET, carbon-13 magic angle spinning line shapes emanating from methylene carbons in PET are used to monitor the conformation of PET in the blends, and indirect detection of ^{1}H spin–lattice relaxation in the rotational frame ($T_{1\rho}$) is used to estimate the crystallinity of the two polymers in blends. We find that these NMR data and previously published results for the same system[3] are consistent with a model in which Vectra can penetrate PET regions within blends upon annealing into the melt.

Experimental Section

Materials. The blends used in this study were composed of Vectra-A 900, a random copolymer of hydroxybenzoic acid (HBA) and hydroxynaphthoic acid (HNA), and poly(ethylene terephthalate) (PET), both supplied by Hoechst Celanese. Blends with various compositions were prepared by single-screw extrusion in the melt and characterized rheologically, by thermal analysis, and by electron microscopy, as described previously.[8] Some samples were annealed at 310 °C for 10 min.

NMR Experiments. Most spectra were obtained on a home-built solid-state NMR spectrometer operating at 25.2 and 100.4 MHz for ^{13}C and ^{1}H resonances, respectively. The magic angle spinning (MAS) experiments were carried out using a Doty VT-MAS probe, while a home-built double-resonance probe was used for static measurements. Both probes have a nominal 90° pulse

0024-9297/93/2226-4269$04.00/0

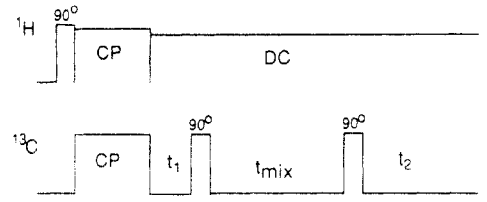

Figure 1. Pulse sequence for 2D rotor-driven ^{13}C spin diffusion experiment.[15]

of 3 μs for ^{1}H and 5 μs for ^{13}C. The recycling delay was set to 15 s for all experiments except for T_1 measurements, in which a recycling delay of 1 min was normally used.

Carbon-13 cross-polarization (CP) MAS NMR experiments were conducted with a CP contact time of 1.5 ms. There were no spinning sidebands at 2-3 kHz sample rotation speeds because of relatively small chemical shift anisotropy at the low field. To assist in the assignment of Vectra chemical shifts, an interrupted decoupling experiment was performed in which the ^{1}H decoupling was turned off for 50 μs prior to data acquisition.

The ^{1}H spin–lattice relaxation in the laboratory frame can be probed indirectly using ^{13}C MAS spectra to achieve higher spectral resolution.[10] In these experiments, the ^{1}H magnetization after the inversion–recovery was first transferred to ^{13}C and then the resulting ^{13}C signal was acquired. The intensities of ^{13}C resonance as a function of ^{1}H recovery time provide the T_1 measurements for protons in the blends.

Proton spin-lock relaxation experiments for $T_{1\rho}$ measurements were performed by applying a resonant spin-lock field phase-shifted 90° relative to the initial exciting pulse. The typical strength of the lock field was 80 kHz. The relaxation of the locked ^{1}H transverse magnetization was detected by measuring the intensity of ^{13}C resonance through cross polarization after various spin-lock times.

The pulse sequence for the two-dimensional rotor-driven ^{13}C spin diffusion experiment is shown in Figure 1. This sequence resembles a conventional 2D spin diffusion pulse sequence[11] except that (i) the ^{1}H decoupling is on during the mixing period and (ii) the sample spinning speed is set to be exactly the same as the resonance frequency *difference* of the two spins between which spin diffusion is expected to occur. In our experiments, the aliphatic carbons of PET and the quaternary carbons of HBA in Vectra were selected to probe the spin diffusion; thus the sample spin speed was set to 2.382 kHz. The spinning speed was stabilized to within 5 Hz. The 2D spectra were usually taken with 32 t_1 increments of 500 μs each. The total number of scans for each t_1 value was 200.

Results

^{13}C Chemical Shifts of Vectra and Vectra/PET Blends. Figure 2 depicts typical high-resolution solid-state ^{13}C CP-MAS NMR spectra of pure Vectra-A, pure PET, and Vectra/PET(50/50) blend. The chemical shifts for different carbons are listed in Table I. For Vectra, unambiguous assignments of the resonance peaks were achieved in two steps, as was done previously[12] for other LCPs. First, two groups of carbons, the protonated and the nonprotonated, were distinguished by carrying out the delayed-^{1}H-decoupling experiments,[13] which suppress effectively the signals from the protonated carbons, resulting in much simplified spectra (not shown) having only resonance peaks 1, 4 (11), 5 (12), 6, and 8. Second, the ^{13}C-NMR spectra of HBA/HNA copolymers were acquired for different HBA/HNA compositions. By comparing relative changes in peak intensities, each peak was further assigned to the HBA moiety or the HNA moiety in Vectra. The same measurements were also carried out on a number of Vectra/PET blends; an example is shown in Figure 2. It should be noted that the ratios of the peak intensities in these spectra do not reflect the compositions in the blends quantitatively due to variations of cross-polarization efficiency of various carbon species. There is no detectable chemical shift difference between the pure

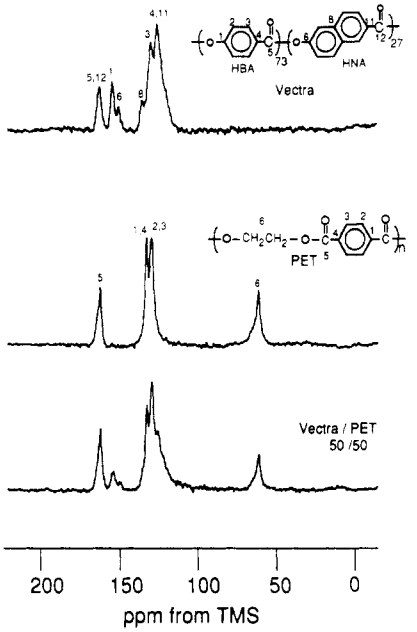

Figure 2. ^{13}C CP-MAS NMR spectra of (a) Vectra-A, (b) PET, and (c) Vectra/PET(50/50) blend.

Table I. Carbon-13 Chemical Shift Assignment for Vectra and PET

Vectra carbons[a]	chem shift (ppm)	PET[a]	chem shift (ppm)
C1	155.9	C1, C4	134.2
C3	130.8	C2, C3	130.6
C4, C11	126.8	C5	164.7
C5, C12	164.8	C6	61.7
C6	151.5		
C8	136.8		

[a] See molecular structures in Figure 2 for carbon numberings.

polymer and the polymer in the blends, as evidenced in Figure 2. This is not surprising; the variation of chemical shifts in copolymers of PET and HBA is not observable by solid-state NMR.[12]

^{1}H Spin–Lattice Relaxation Detected by ^{13}C NMR. Although the ^{13}C chemical shift itself does not provide direct information about the interaction between Vectra and PET, the high spectral resolution achievable in ^{13}C-NMR can be used to probe the behavior of the two polymers in the blends. Previous studies[5,14] have concluded that Vectra and PET are in separate phases in their blends, irrespective of which component is dominant. Our ^{13}C-detected ^{1}H spin–lattice relaxation experiments further demonstrate that these two polymers are, in most cases, immiscible. As revealed in Figure 3, the proton magnetization of PET, represented by the aliphatic carbon intensity at 61.7 ppm, relaxed faster ($T_1 \sim 2.1$ s) than that of Vectra ($T_1 \sim 15$ s), represented by the resonance of quaternary carbons at 155.9 ppm. If Vectra and PET were homogeneously mixed at the molecular level, proton spin diffusion would force the relaxation rates of the protons in the two polymers to be same; the fact that they relax at very different rates is a strong indication of immiscibility. However, when the 50/50 Vectra/PET blend was annealed at 310 °C for 10 min, we observed a biexponential relaxation decay for the PET aliphatic protons, as typified by the data shown in Figure 4. The fast component corresponds to a relaxation rate similar to that of unannealed samples, whereas the T_1 value (~12 s) of the slow component is much larger than that of the unannealed sample (2.1 s) and is only slightly smaller than that of protons in pure Vectra (~15 s). This slow component comprises approximately 7% of the aliphatic protons, as determined by a biexponential fit to the data.

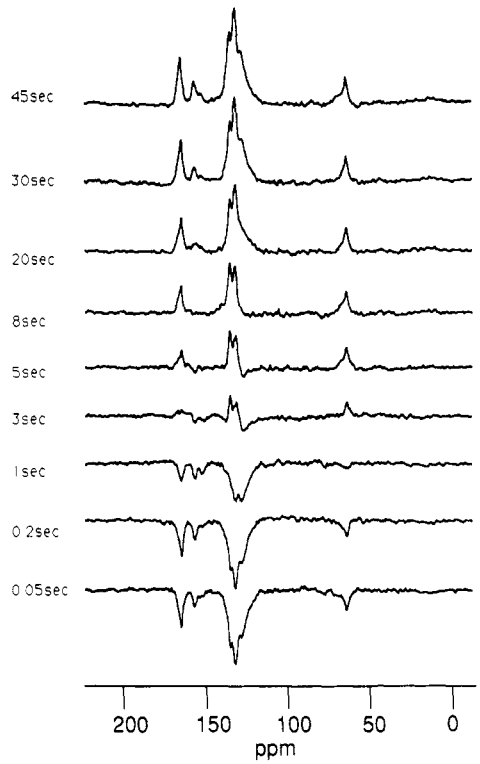

Figure 3. Proton inversion-recovery ^{13}C CP-MAS spectra of Vectra/PET(50/50) blend as a function of the recovery period τ.

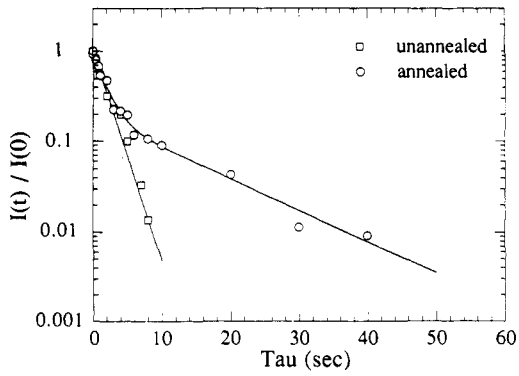

Figure 4. Aliphatic proton intensity (reflected by aliphatic carbon) of PET as a function of the inversion-recovery time. The solid line is the best fit of the data based upon a two-exponential decay.

Rotor-Driven 2D Spin Diffusion Experiment. Two-dimensional ^{13}C spin diffusion experiments have been employed to characterize microscopic homogeneity in disordered solids.[11] Because the spin diffusion rates depend strongly on the distance between nuclei, spin diffusion is confined to neighboring molecules; i.e., if spin diffusion can be observed between two species, they must be mixed intimately on the molecular level. Therefore, the spin diffusion experiment is a powerful tool to determine whether or not intimate mixtures of Vectra and PET exist in our blends.

For natural-abundance ^{13}C samples, the carbon-13 homonuclear dipole–dipole interaction is weak and thus the ^{13}C spin diffusion rate is expected to be low. Indeed, in a conventional 2D experiment we found that the mixing period must be on the order of 30 s or longer to observe all the possible ^{13}C spin diffusion from carbon resonance *within* PET molecules. The total experimental time to observe spin diffusion *between* molecules was therefore unacceptably long. In a rotor-driven spin diffusion experiment, however, the homonuclear "flip-flop" process is coupled to the sample rotation, making spin diffusion considerably more efficient.[15,16] As a result, the diffusion

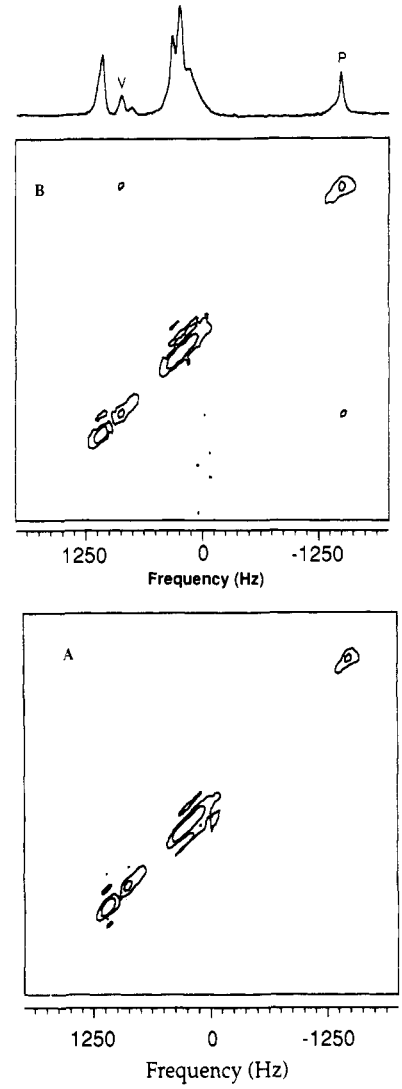

Figure 5. 2D rotor-driven ^{13}C spin diffusion spectra of annealed Vectra/PET(50/50) blend: (A) unannealed sample; (B) annealed sample. The one-dimensional ^{13}C MAS is shown at the top with aliphatic PET resonances (P) and quaternary Vectra-A resonances (V) marked for clarity.

rates are increased by several orders of magnitude, and the mixing time thus can be reduced dramatically.

Figure 5 shows a 2D rotor-driven ^{13}C spin diffusion spectrum obtained with the pulse sequence shown in Figure 1 for both annealed and unannealed 50/50 Vectra/PET blends. The data for the unannealed sample (Figure 5A) do not exhibit cross peaks between the aliphatic carbons of PET and the quaternary carbons of HBA in Vectra. It is important to note that experiments run under similar conditions with pure PET show cross peaks between carbon resonances *within the same molecule*. After annealing the PET/Vectra-A blend at 310 °C for 10 min, however, the spectrum shown in Figure 5B emerges. Even with a mixing time of only 300 ms, cross peaks for the aliphatic (PET) and quaternary (Vectra) carbons are present. The occurrence of the cross peaks indicates unambiguously the existence of intimate molecular mixing of Vectra and PET after annealing.

Blending Effects on the Line Shape. The blend composition and thermal history have pronounced effects on the observed line shape of methylene carbons of PET in the blends, as shown in Figures 6 and 7. In general, the methylene carbon resonance of PET has an asymmetric line shape which comprises two components: a narrow component to higher field (right) and a broad one to lower field (left). Previous workers[17] have assigned the former to methylene carbons in the *trans* conformation, and the

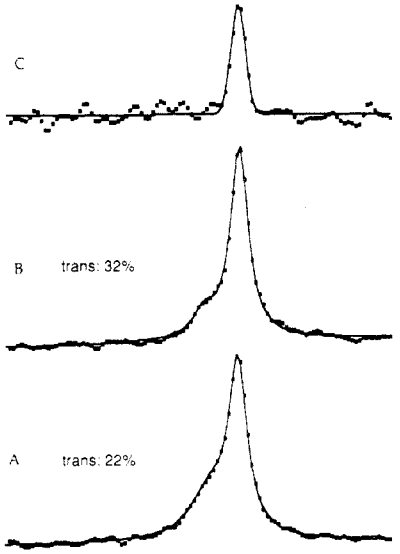

Figure 6. Methylene carbon resonance peaks for (A) unannealed Vectra/PET(10/90) blend, (B) annealed Vectra/PET(10/90) blend, and (C) the narrow component of annealed Vectra/PET-(10/90) blend obtained after 50-ms proton spin lock. Dots are experimental data, and the solid line is a fit based on the combination of Gaussian and Lorentzian functions.

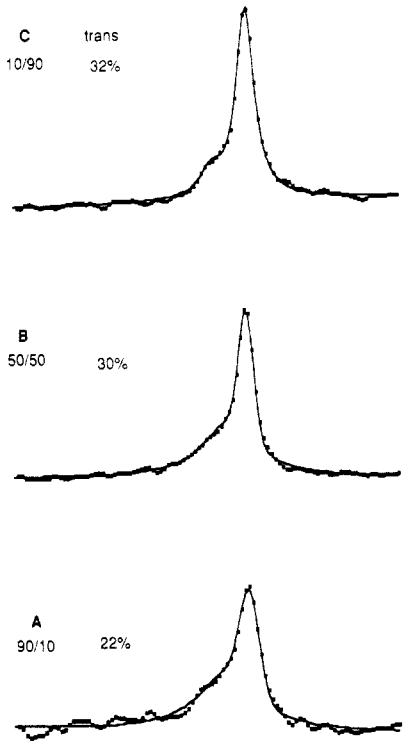

Figure 7. Methylene carbon resonance peaks for the blends of different composition: (A) Vectra/PET(90/10); (b) Vectra/PET-(50/50); (C) Vectra/PET(10/90). Dots are experimental data, and the solid line is a fit based on the combination of Gaussian and Lorentzian functions.

latter to carbons in the *gauche* form.

The chemical shift difference, the line widths, and the relative ratios of the two components were resolved through computer fittings of the peaks. The overall resonance peak is well fit to the sum of a Lorentzian function for the narrow component and a Gaussian for the broad component. The chemical shift difference of these two components is about 1 ppm, which is close to that observed previously in pure PET.[17] The dependencies of the line width and the fraction of the two components on the thermal history are reflected in spectra B and C of Figure 6, respectively. Assuming no changes in the time constants associated with cross polarization, so that relative intensities are representative of concentrations, we see that the relative amount

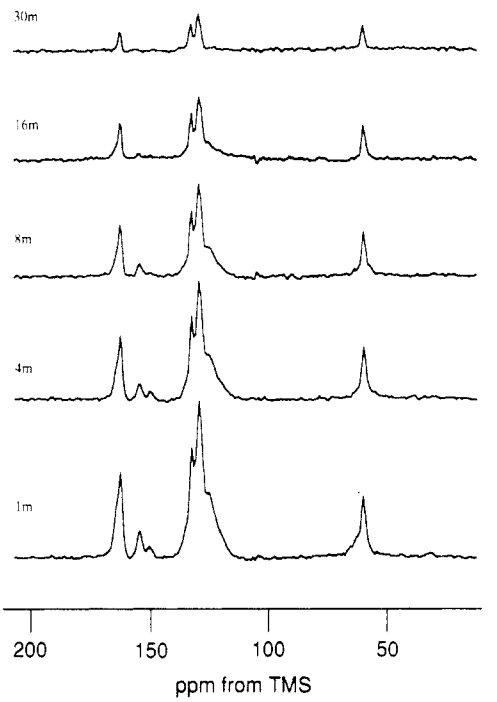

Figure 8. ^{13}C CP-MAS spectra with different ^{1}H spin lock times, given in milliseconds.

of *gauche* conformer is reduced greatly upon annealing; the line width of the broad resonance also becomes narrower after annealing. This is consistent with previous conclusions where annealing above the glass transition temperature allows conformations at the methylene linkages to change from *gauche* to *trans*. Samples with the same thermal history but different blend compositions are compared in Figure 7. It is clear that *gauche* conformers are preferred in blends containing low mole fractions of PET.

$T_{1\rho}$ Measurement and Crystallinity. The crystallinity of PET and Vectra can be estimated through the measurement of rotating frame spin–lattice relaxation times, $T_{1\rho}$, which are sensitive to molecular motions with characteristic frequencies of 1–50 kHz. For polymer blends, one of the advantages of $T_{1\rho}$ measurement over other techniques, such as X-ray diffraction, is that individual components of the polymer can be resolved. As shown in Figure 8, the ^{1}H rotating frame relaxation of protons associated with both Vectra and PET can be monitored separately by observing the methylene carbons at 61.7 ppm for PET and the quaternary carbons at 155.9 ppm for Vectra.

Figure 9 depicts the intensity decay for protons associated with the methylene carbons at 61.7 ppm in PET for annealed and unannealed blends as a function of spin lock time. The data were fit well with biexponential decay functions. The annealed blend has a higher percentage of long $T_{1\rho}$ component, suggesting an increase in PET crystallinity. Data for protons associated exclusively with Vectra showed no obvious changes in the amount of crystallinity; this is consistent with unpublished X-ray diffraction results in our laboratory[18] in which pure Vectra and a blend of 0.9 weight fraction of Vectra with PET do not show any significant difference in their diffraction patterns before and after annealing.

It is important to note the correlation between blend composition and crystallinity of each polymer. Figure 10 shows rotating frame relaxation data for protons associated with the methylene carbons at 61.7 ppm in PET samples with the same annealing conditions but for samples of different composition. Obviously, the PET protons relax at a faster rate in the blends with lower PET weight

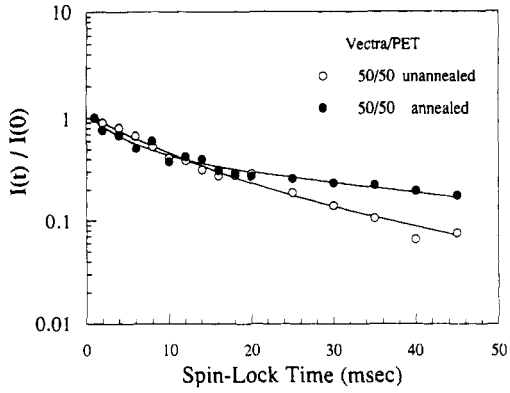

Figure 9. ^{1}H rotating-frame relaxation data of PET in the Vectra/PET(50/50) blends, which was detected by methylene carbon signals. For the unannealed 50/50 blend, $T_{1\rho}$ = 7.6 ms (66%) for the short component and $T_{1\rho}$ = 26.8 ms (34%) for the long component. For the 50/50 annealed blend, $T_{1\rho}$ = 4.5 ms (59%) for the short component and $T_{1\rho}$ = 46.4 ms (41%) for the long component.

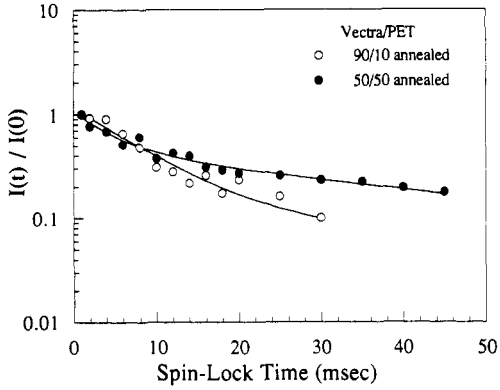

Figure 10. ^{1}H rotating-frame relaxation data of PET in the Vectra/PET blends with different compositions. For the 90/10 annealed sample, $T_{1\rho}$ = 7.7 ms (91%) for the short component and $T_{1\rho}$ = 67.6 ms (9%) for the long component.

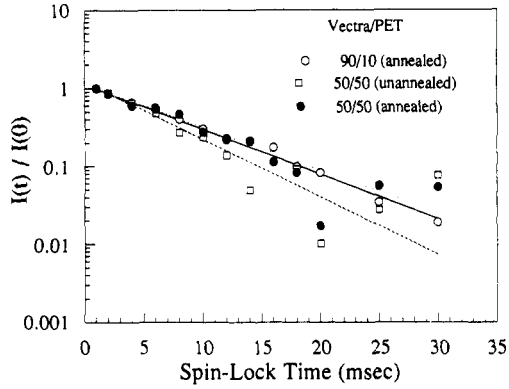

Figure 11. ^{1}H rotating-frame relaxation data of HBA in the blends, which was detected by the quaternary carbon signals of HBA. The solid line shows the best fit to the data based on an exponential decay. The $T_{1\rho}$ values of each sample were calculated from the fitting results: (a) annealed Vectra/PET(90/10), $T_{1\rho}$ = 7.9 ms; (b) annealed Vectra/PET(50/50), $T_{1\rho}$ = 7.6 ms; (c) unannealed Vectra/PET(50/50), $T_{1\rho}$ = 5.7 ms.

fraction. Contrarily, data for protons associated with Vectra showed a constant relaxation rate in the blends of differing composition (Figure 11).

Discussion

The present NMR studies and previous work[3] are consistent with a model for the Vectra/PET interface in which annealing allows for penetration of Vectra into the PET regions, but not vice versa. We argue below that the spin diffusion and laboratory frame relaxation measurements establish mixing, the rotating frame experiments establish how the crystallinity of each component is affected by blending and annealing, and the methylene resonances associated with PET establish the role *gauche* conformers play at the Vectra/PET interface.

Mixing of Vectra and PET. Blends of rigid rods and flexible chains are thermodynamically immiscible. The Vectra-A chain is not rigid, but the difference in chain flexibility of Vectra and PET is large enough to cause the two polymers to phase separate. The immiscibility of Vectra and PET has been established in the unannealed blends through ^{13}C-detected ^{1}H spin–lattice T_1 measurements. A single T_1 value would be observed if the two molecules mixed homogeneously on a microscopic scale.[10] The completely different T_1 relaxation rates for protons associated with Vectra and PET in the blends indicate that they are not mixed at the molecular level.

Annealing into the melt state results in significant changes in NMR data. Laboratory frame proton spin–lattice relaxation measurements (Figure 4) and 2D spin diffusion spectra (Figure 5) indicate the existence of interactions in the annealed Vectra/PET blends. Figure 4 shows that the long T_1 components, which may come from a miscible phase, occurs *only* in the annealed blends. Figure 5 further demonstrates that a miscible phase exists in the annealed blends. The spin diffusion of carbon-13 can be detected only within a distance of 1 nm or less,[19,20] due to the low concentration of ^{13}C spins and the strong dependence on nuclear separation ($1/r_{ik}^6$). The cross peaks in Figure 5 which connect the resonances of Vectra and PET unambiguously demonstrate that Vectra and PET can form a homogeneous phase in the annealed samples.

There are at least two processes that can cause Vectra and PET to mix microscopically in the annealed blends. Some interdiffusion might occur despite the unfavorable thermodynamics, since Vectra is not perfectly rigid. Transesterification, a chemical reaction between polyesters, is also a possibility. Transesterification has been observed in the blend of poly(HBA/PET) and polycarbonate after annealing in the melt state.[6] Transesterification in liquid crystalline polyester blends was found to dramatically improve miscibility of blends.[21,22] Our attempts to establish whether or not chemical reaction occurred, for example by polymer dissolution in strong acids followed by analysis of high-resolution ^{13}C NMR spectra, were unsuccessful. We doubt, however, that measurable transesterification occurs after annealing for only 10 min at 310 °C. The data shown in Figures 4 and 5, however, cannot exclude either possibility, or a combination of both.

Annealing Effects on Polymer Conformation and Crystallinity. Annealing at 310 °C affects the crystallinity and molecular conformation of the PET component in the blends but has little effect on the Vectra component. Rotating frame proton ($T_{1\rho}$) relaxation measurements show that annealing increases the crystallinity of the PET fraction while it does little to change the crystallinity of the Vectra fraction. The decrease in *gauche* conformer relative to *trans* in PET after annealing, as reflected in the line shape of methylene carbon resonance (Figure 6), is consistent with an increase in crystallinity of the PET since the reduction of *gauche* conformation after annealing is associated with a decreasing fraction of amorphous material.

Inspection of Figure 8 shows that the broad component of methylene resonance decays faster under proton spin-lock conditions than the narrow component. Therefore we associate the short $T_{1\rho}$ (fast decaying) component with *gauche* PET conformers, which in turn emanate from amorphous regions of PET. Figure 9 shows that this component decays faster upon annealing, indicating that

annealing affords increased molecular motion in the regions of the polymer associated with *gauche* conformers. If we associate the *gauche* conformers with the amorphous PET at the Vectra interface, then penetration of the PET by Vectra upon annealing could afford more motional degrees of freedom and thereby increase segmental motional and decrease $T_{1\rho}$. This result is in contrast to what has been found in the pure PET system,[17] where $T_{1\rho}$ becomes longer upon annealing. It is believed that in pure PET, the formation of many small crystallites, which can act as cross-links, inhibits the cooperative segmental motion in the amorphous region.[23]

Changes in PET conformation and crystallization as a function of blend composition are displayed in Figures 7 and 10, respectively. The smaller the weight fraction of PET in the blends, the more PET is in the *gauche* form (Figure 7). The long $T_{1\rho}$ component of the aliphatic protons, representing PET crystallites in the blends, was greatly reduced in the Vectra/PET(90/10) blend compared to the Vectra/PET(50/50) blend (Figure 10). These variations can be interpreted in terms of blend texture. In the Vectra-dominated blends PET appears as spheres embedded in the Vectra matrix.[3] This results in a high surface-to-volume (s/v) ratio for PET. As Vectra and PET approach equal amount in the blends, continuous phases with relatively low s/v are formed. When PET becomes dominant in the blends, the s/v ratio for PET is even lower. The concomitant tendency of more *gauche* form and larger s/v ratio in blends of low PET content implies that the *gauche* form is preferred at the Vectra/PET interface, which is in agreement with a recent prediction.[24]

Correlation between Intimate Mixing and Thermal Behavior of Blends. If a crystalline polymer is surrounded by a melt which contains impurities, the melting point of the crystallites will decrease.[25] This is readily understandable because the melting point, by definition, is the temperature at which the chemical potentials of the polymer repeating unit in the two phases are equal. Introduction of impurities to the liquid phase decreases the chemical potential in this phase; to reestablish the condition of equilibrium, a lower melting temperature T_m is required. The same argument can be applied to the crystallization temperature T_c.

Previous differential scanning calorimetry (DSC) measurements[3] showed the depression of melting and crystallization temperatures (T_m and T_c) in the PET phase of annealed blends. The extent of the depression depended on the blend composition and the annealing times. The lower the PET weight fraction and the longer the annealing time, the greater is the extent of depression of the transition temperatures. As noted earlier, both the spectral analyses of the methylene carbon resonance and the ^1H $T_{1\rho}$ measurements suggest more *gauche* conformers at the Vectra–PET interface, where PET appears as amorphous. Because *gauche* conformers have relatively large free volume, it is conceivable that Vectra can diffuse into the amorphous regions of PET during melting and act as "impurities". Assuming that this is the case, then a larger surface-to-volume ratio, corresponding to lower PET fraction, and longer annealing time will allow more Vectra to diffuse into PET, leading to a higher impurity content in the amorphous regions of PET and lower transition temperatures in the pure PET phase. The same argument also explains why the transition temperatures of Vectra in PET-dominant blends are not depressed significantly. At the annealing temperature of 310 °C, Vectra is in the nematic phase, which has a much smaller free volume due to the alignment of molecular chains. Consequently, little PET can diffuse into Vectra and the depression of Vectra transition temperature is not observable.

Conclusions

There exists a miscible component in our annealed Vectra/PET blends as indicated by the NMR measurements. The intimate mixtures amount to about 7% of the total in the 50/50 Vectra/PET blend, which has been annealed for 10 min at 310 °C. The average distance between the aliphatic carbons of PET and the quaternary carbons of Vectra is less than 1 nm in the intimately blended regions. The transesterification of PET and Vectra is also possible in these regions after long annealing at high temperature. The intimate mixtures most likely exist at the interface of Vectra and PET, because more *gauche* conformers of PET are near the surface. The existence of the intimate mixture affects the thermal behavior of the blends, such as the depression of T_m and T_c of PET.

Acknowledgment. We wish to thank Professor G. Harbison, Dr. T. Barbara, and Dr. Ron Haner for allowing us to use their NMR instruments for pilot experiments. This work was supported in part by the Director, Office of Energy Research, Office of Basic Energy Science, Materials Science Division, U.S. Department of Energy, under Contract No. DE-AC03-76SF00098 and in part by a gift from IBM.

References and Notes

(1) National Research Council *Liquid Crystalline Polymers*, Report of the Committee on Liquid Crystalline Polymers, NMAB-453; National Academy Press, Washington, 1990.
(2) Dutta, D.; Fruitwala, H.; Kohli, A.; Weiss, R. *Polym. Eng.* **1990**, *30*, 1005–1018.
(3) Kim, W. N.; Denn, M. M. *J. Rheol.* **1992**, *36*, 1477–1498.
(4) Lee, W. C.; Dibenedetto, A. T. *Polym. Eng. Sci.* **1992**, *32*, (6), 400–408.
(5) Sharma, S. K.; Tendolkar, A.; Misra, A. *Mol. Cryst. Liq. Cryst. Inc. Nonlin. Opt.* **1988**, *157*, 597–614.
(6) Kosfeld, R.; Hess, M.; Friedrich, K. *Mater. Chem. Phys.* **1987**, *18*, 93.
(7) Silverstein, M. S.; Hiltner, A.; Baer, E. *J. Appl. Polym. Sci.* **1991**, *43*, 157–173.
(8) Parmer, J. F.; Dickinson, L. C.; Chien, J. C. W.; Porter, R. S. *Macromolecules* **1987**, *20*, 2308–2310.
(9) VanderHart, D. L. *Makromol. Chem., Macromol. Symp.* **1990**, *34*, 125–159.
(10) Tang, P.; Juang, C. L.; Harbison, G. S. *Science* **1990**, *249*, 70–72.
(11) Caravatti, P.; Deli, J. A.; Bodenhausen, G.; Ernst, R. R. *J. Am. Chem. Soc.* **1982**, *104*, 5506–5507.
(12) Amundson, K. R.; Reimer, J. A.; Denn, M. M. *Macromolecules* **1991**, *24*, 3250–3260.
(13) Opella, S. J.; Frey, M. H. *J. Am. Chem. Soc.* **1979**, *101*, 5854.
(14) Perkins, W. G.; Marrcelli, A. M.; Frerking, H. W., Jr. *J. Appl. Polym. Sci.* **1991**, *43*, 329–349.
(15) Colombo, M. G.; Meier, B. H.; Ernst, R. R. *Chem. Phys. Lett.* **1988**, *146*, 189.
(16) Levitt, M. H.; Raleigh, D. P.; Creuzet, F.; Griffin, R. G. *J. Chem. Phys.* **1990**, *92*, 6347–6364.
(17) Sefcik, M. D.; Schaefer, J.; Stejskal, E. O.; Mckay, R. A. *Macromolecules* **1980**, *13*, 1132–1137.
(18) Kim, W. N., unpublished.
(19) Spiess, H. W. *Chem. Rev.* **1991**, *91*, 1321–1338.
(20) Bernhard, B. *Adv. Mater.* **1991**, *3*, 237–244.
(21) George, E. R.; Porter, R. S. *Macromolecules* **1986**, *19*, 97–105.
(22) George, E. R.; Porter, R. S. *J. Polym. Sci., Polym. Phys. Ed.* **1988**, *26*, 83–90.
(23) Illers, K. H.; Breuer, H. *J. Colloid Sci.* **1963**, *18*, 1.
(24) Biswas, A.; Schurmann, B. L. *J. Chem. Phys.* **1991**, *95*, 5377–5386.
(25) Flory, P. J. *Principles of Polymer Chemistry*; Cornell University Press: Ithaca, NY, 1953.